Experimental Thermal and Fluid Science 85 (2017) 279–286

Contents lists available at ScienceDirect

Experimental Thermal and Fluid Science

journal homepage: www.elsevier.com/locate/etfs

Dynamics of a thin liquid film under shearing force and thermal influences

Ke Wang [a,b], Youjia Zhang [b], Shengjie Gong [c], Bofeng Bai [d], Weimin Ma [b,*]

[a] Beijing Key Laboratory of Process Fluid Filtration and Separation, China University of Petroleum, Beijing 102249, China
[b] Department of Physics, Kungliga Tekniska Högskolan (KTH), Stockholm 10044, Sweden
[c] School of Nuclear Science and Engineering, Shanghai Jiao Tong University, Shanghai 200240, China
[d] State Key Laboratory of Multiphase Flow in Power Engineering, Xi'an Jiaotong University, Shaanxi 710049, China

ARTICLE INFO

Article history:
Received 4 October 2016
Received in revised form 13 February 2017
Accepted 5 March 2017
Available online 7 March 2017

Keywords:
Stratified flow
Liquid film dynamics
Instability
Film rupture
Shear force

ABSTRACT

Study of liquid film dynamics promotes understanding the critical heat flux (CHF) of boiling heat transfer, which occurs as the liquid layers (micro-layer and macro-layer) near the heater wall lose their integrity. Since the measurement at micro-scale is a challenge, and further complicated by the chaotic nature of the boiling process, profound knowledge on the thin liquid film dynamics is not well documented in the existing literature. In the present paper, we employ a confocal optical sensor system to study the dynamics and the integrity of a thin liquid film sheared by the co-flowing air from above and heated from below in a horizontal aluminum channel. The results indicate that the entrainment governs the liquid film thinning process under adiabatic or lower heat flux conditions, whereas the evaporation becomes more pronounced in a higher heat flux system. The detailed evolution of liquid film is discussed. Based on our experimental observations, the critical film thickness of an integral film is related to the condition of the heating surface and the heat flux. For a specific surface, the critical film thickness remains constant under a defined heat flux and increases with the increasing heat flux. A spectrum analysis is also implemented to analyze the film instability. It is concluded that the heat flux is the dominant factor to govern the film instability compared with the effect of differential velocities of gas and liquid flow.

1. Introduction

A thin liquid film spreading over and evaporating on a solid surface is encountered in many engineering applications that involve processes such as spray cooling, heating, coating, cleaning and lubrication. In most cases, the stability and integrity of the liquid film on the heating surface is desired to avoid performance deterioration and physical destruction of the devices. Note that the performance of a boiling device is bounded by the critical heat flux (CHF), which is thus an important parameter for system design and operation [1]. If the liquid film rupture occurs in boiling heat transfer, for instance, the heat transfer coefficient may be considerably reduced and it will lead to the burnout (dryout) which is a threat to the equipment safety.

So far, an extensive research has been carried out in the investigation the liquid film dynamics and integrity. The minimum thickness of an integral liquid film is of special interest since it is related to film rupture. For adiabatic conditions, the minimum thickness of the film flowing down a vertical or inclined solid surface can be predicted theoretically according to force balance or minimum total energy criteria [2–7], as well as a horizontal liquid film by free energy theory [8,9]. Oron et al. [10] provided a comprehensive review of the multifaceted subject of thin film dynamics modeling. Based on the long wave theory, they presented a unified mathematical system to predict the long-scale evolution of thin liquid films. The set of mathematical evolution equations has its root in the work of Burelbach et al. [11], taking into account the influential factors such as van der Waal forces, surface tension, gravity, thermo-capillary, mass loss and vapor recoil force. Later, Craster and Matar [12] also presented a comprehensive review of the work carried out on thin film flows. As pointed out by Oron et al. [10], there is a clear need for careful experimental investigations to verify phenomena and to give data that can be used to test the theories, and they claimed their review paper stands as a call for such experiments. Remarkably, there are few data for film rupture on a horizontal surface under non-adiabatic conditions which is important to boiling heat transfer and boiling crisis.

Additionally, most of the published modeling and numerical studies for boiling heat transfer concentrate on the near-wall liquid

* Corresponding author.
E-mail address: weimin@kth.se (W. Ma).

http://dx.doi.org/10.1016/j.expthermflusci.2017.03.014
0894-1777/

Nomenclature

f	frequency (Hz)
M_l	liquid mass flow rate (g/s)
q	heat flux (kW/m^2)
t	Time (s)
u_m	mixture velocity (m/s)
u_{sg}	gas superficial velocity (m/s)
u_{sl}	liquid superficial velocity (m/s)
x	axial distance (mm)

Greek letters

δ	film thickness (mm)

Subscripts

g	gas
l	liquid

layers (micro/macro-layer) with the thickness estimated to range from several to hundred micrometers [13–17]. However, there is a dearth of data on the direct measurement of such near-wall liquid layers. This is probably due to the fact that the measurement at micro-scale is a challenge, and further complicated by the traditional experimental setups (e.g. Pool boiling with heater block) and the chaotic nature of boiling process which all impede direct observation and measurement of thin liquid films, especially under high heat-flux conditions.

Theofanous et al. [18,19] proposed a "scales-separation" phenomenon which indicates that high heat-flux boiling and boiling crisis is dominated by micro-hydrodynamics of liquid microlayer on the heater surface. More specifically, for a given surface condition and coolant chemistry, boiling crisis can be treated as a hydrodynamic phenomenon, and there exist two hydrodynamic scales: an external one and an internal one. However, boiling crisis in pool boiling is irrelevant to the external-scale hydrodynamics. Note that the "scales-separation" phenomenon can also be applied to flow boiling [20]. This provides the rationale to perform the BETA-B boiling experiment [21] on a thin liquid film so that the micro-hydrodynamics of the film was visualized directly by a high-speed video camera synchronized with the IR imaging, without losing the key physics of boiling. To take one step forward, Gong et al. [22,23] developed an experimental method for the diagnosis of liquid film dynamics and investigated the stability and rupture of evaporating liquid films on different heater surfaces under boiling conditions from low heat fluxes to high fluxes [24–26]. The data were then applied in the modeling and simulation of liquid film dynamics [27]. Since previous studies were oriented to pool boiling, there is a clear need to advance the developed experimentation to flow boiling so that the research is applicable to boiling water reactors. Note that the flow boiling features a liquid film driven by shear forces of vapor flow in the mainstream. The shear force not only affects the instability of the micro-layer, but also forces the liquid in the micro-layer to spread into the dry areas. Generally, the interfacial waves on the liquid film is believed to trigger the dryout in flow boiling [28]. However, the experimental quantification of such thin liquid films and their dynamics is not straightforward. Essentially, more experimental data and in-depth analysis are required to investigate the film rupture.

The present study calls into question the effects of gas shearing and evaporation on the dynamics of a thin liquid film. We develop a confocal optical sensor system for a rapidly varied liquid film and try to evaluate the factors and properties which govern film dynamics, stability and rupture. We discuss the effects of entrainment and evaporation on liquid film evolution. We also analyze the effects of different parameters (e.g. gas and liquid flow rate, heat flux, etc.) on the critical film thickness. Based on the spectrum analysis, we discuss the film instability under various flow conditions, providing insights into the dynamics of a thin liquid film.

2. Experimental system and method

2.1. Test facility

Fig. 1 shows the schematic of the test facility which mainly consists of water and air supply systems, a heating system, a test section as well as a measurement system. The test section is a rectangular channel made of aluminum with the length of 180 mm, the width of 8 mm and the height of 12 mm, as seen in Fig. 2. In order to isolate the vibration, the test facility is fixed on an optical table which also serves as an operating platform to fix the test section horizontally. The surface of the test channel has the properties of 0.293 Ra/μm for roughness and 68° for contact angle. For the purpose of forming a stratified flow with minimum entrance effect, a water-air inlet section is carefully designed to make water and air flow into the test section in parallel.

The main difficulties for the dynamics of the thin liquid film measurement are the film's small scale and rapid evolution, as well as randomness of nucleation and bubble growth. For a rapidly varied liquid film, the confocal optical sensor is employed because the sensor is equipped with a data acquisition rate up to 30 kHz, and able to measure thickness ranging from several μm to 3 mm with nominal spatial resolution up to less than 1 μm. In the present study, the confocal optical sensor, fixed on a linear guide system (Igus, model DryLin), is incorporated with a controller (optoNCDT2431) which is also connected to a special Xenon light source. By detecting the reflections from the upper and the lower surfaces of the liquid film, the film thickness can be efficiently and accurately deduced. The detailed principle of the confocal optical sensor is accessible in [22].

A copper block with imbedded six cartridge heaters (CIR-30224 230 V 400 W) is employed as the heat source attached to the downward surface of the metallic test sections, which can provide up to 4 MW/m^2 heat flux to the liquid film. The power level of the cartridge heaters is regulated by a DC power transformer and the temperature profile of the copper block is monitored by K-type thermocouples. In order to eliminate condensation of vapor on the upper surface, an AC heater power supply is applied to preheat the air flow before it enters the test section.

2.2. Experimental method and procedures

For adiabatic tests, the water and air are supplied separately to the water-air inlet section at room temperature to form a stratified flow. For boiling tests, de-ionized water is firstly degassed about 30 min and then cooled down to the room temperature. Afterwards, water is circulated by the pump to the test section and compressed air is also provided to the channel after filtering and pre-heating. When the flow becomes stable at the given liquid and air flow rates and heat flux, the confocal optical sensor is operated to measure the dynamic liquid film thickness profiles along

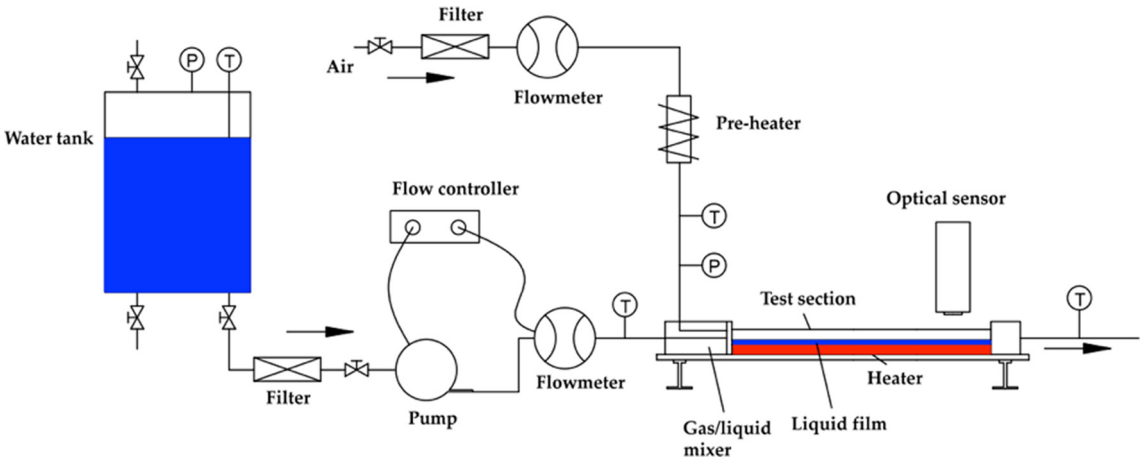

Fig. 1. Schematic of test facility.

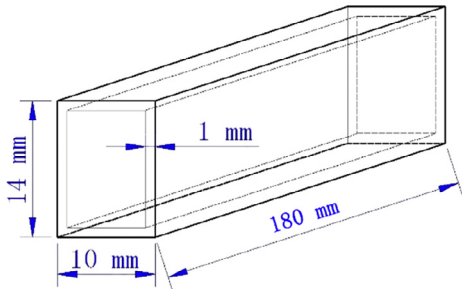

Fig. 2. The dimensions of test section.

the longitudinal (x-axis) and transverse (y-axis) directions. Fig. 3 shows the distribution of the preliminary measurement points (3×5) on the test channel surface. Note that the measurement points locate at least 135 mm away from the inlet of the channel, which insures that the measurements are corresponding to the fully developed equilibrium stratified flow.

For each test run, the liquid film thickness is recorded by sampling rate of 1000 Hz over a period of 60 s. In the present study, the gas velocity ranges from 0.31 m/s to 5.02 m/s, the liquid mass flow rate ranges from 0.03 g/s to 0.30 g/s and heat flux ranges from 0 kW/m^2 to 109 kW/m^2. It is noted that all the experiments are carried out under the atmospheric pressure.

2.3. Data processing

Note that the optical sensor is sensitive to capture the details of film fluctuation. Fig. 4a shows the typical time-trace of film thickness with the periodic fluctuation obtained by the optical sensor. It is noted that the raw signals acquired from the transducer contain substantial background noise (e.g. ambient vibration and natural frequency of pump). Thus, the fast Fourier transform algorithms (FFT) is employed to reduce noise before liquid film features are extracted (see Fig. 4b).

Due to the gas shearing and evaporation, the liquid film decreases along the flow direction. However, the optical sensor will not work well when film rupture occurs, as seen in Fig. 5. The minimum film thickness of an integrated film is defined as the critical film thickness. Since the occurrence of the film rupture is random, five tests are repeated to obtain the averaged critical film thickness and rupture frequency.

2.4. Uncertainty

The air flow rate is measured by the mass flowmeter Vögtlin-GSCC5TSBB1 with the uncertainty of 0.3%, and the liquid mass flow rate by a Coriolis mass flowmeter YOKOGAWA RCCF31DH2MPSIE1 with the uncertainty of 0.5% and the temperature by K-type thermocouples with an accuracy of 1 K. In addition, a liquid flow rate controller Fluidwell F120 is used to ensure a more stable liquid flow rate. The characteristics of the confocal optical sensor are listed in Table 1. For the demonstration of the reliability and feasibility of the confocal optical sensor for thickness measurement, a set of gauge blocks (Mitutoyo, Class 0 with the accuracy of ±0.4 μm) is employed to calibrate the optical sensor before the tests. It can be inferred from Fig. 6 that the optical sensor is capable of measuring the thicknesses of the gauge blocks with a root-mean-square deviation (RMSD) of 9.5%.

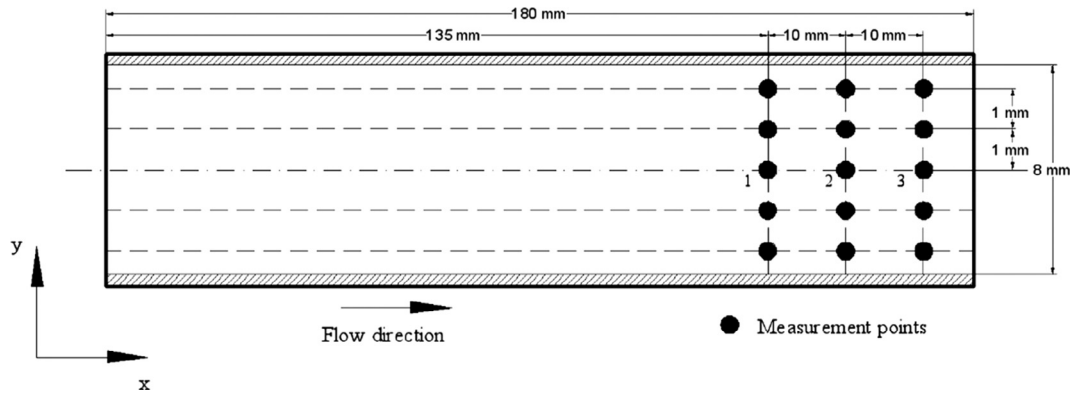

Fig. 3. The distribution of measurement points.

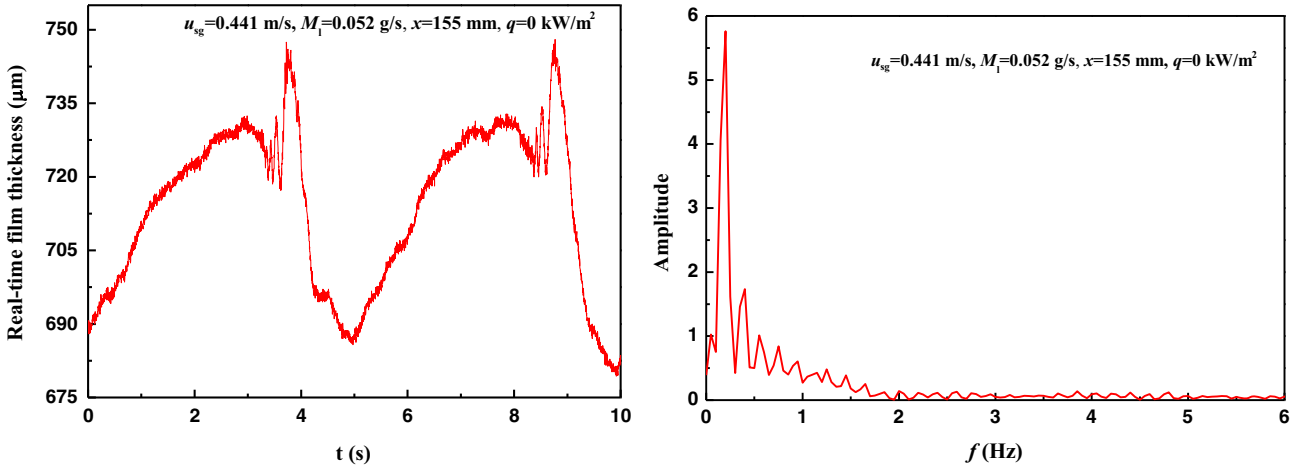

(a) Typical time-trace film thickness. (b) Spectrum of liquid film.

Fig. 4. Time series and spectrum analysis of the film wave signals.

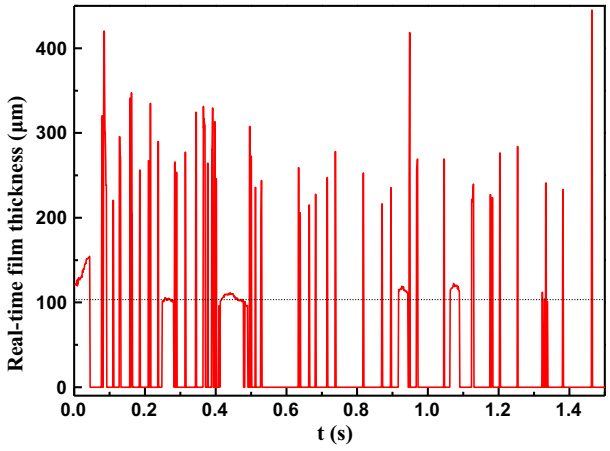

Fig. 5. Typical detected film thickness when film rupture occurs.

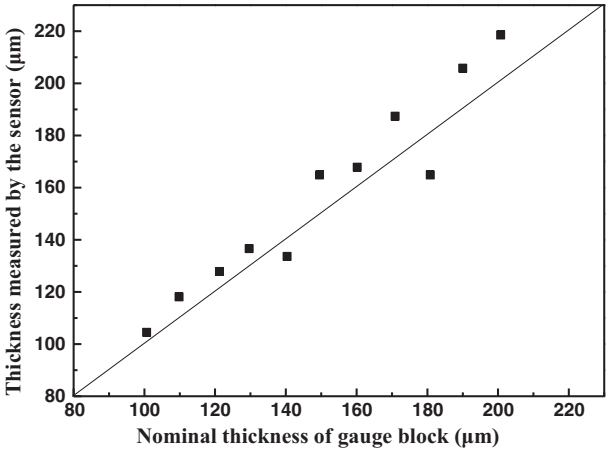

Fig. 6. Calibration of the optical sensor.

Fig. 7 shows a typical distribution of liquid film in axial and transverse directions. The liquid film decreases along the flow direction and its transverse profiles show a concave shape which is approximate symmetrical distribution. Thus, the thinnest part of an integrated liquid film is believed to appear near the outlet of the test channel around the central line. For a simplification, three measurement points (numbered 1–3 in Fig. 3) are finally selected in the present study.

It is known that the increasing heat flux results the promotion of bubble generation. Generally, when the liquid film is thick, the effect of bubble generation on thickness measurement can be ignored and the measured film thickness under non-adiabatic condition is believed to be smaller than that in adiabatic scenario due to the evaporation (region I in Fig. 8). Since the increasing gas velocity leads to a decrease in film thickness, the effect of bubble generation and departure gradually enhanced. Fig. 9 shows the detected departure of the bubble by the optical sensor, which causes a faster and larger amplitude of vibration of the liquid film.

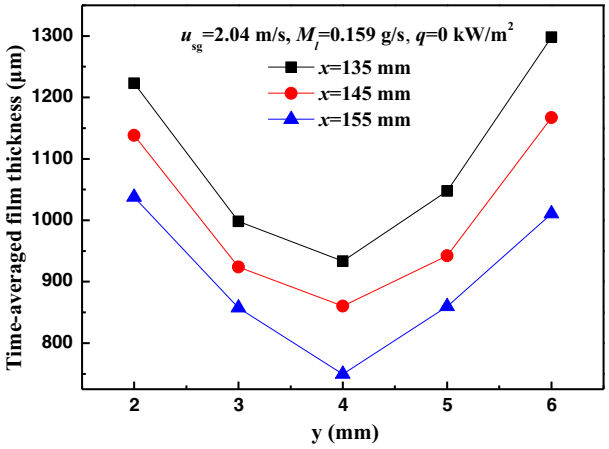

Fig. 7. The liquid distribution in axial and transverse directions.

Table 1
The parameters of the optical sensor.

Sensor model	Measuring range	Spot diameter	Resolution	Max. tilt
IFS2431-3	3 mm	25 μm	0.12 μm	± 22°

Remarkably, the growth of the bubbles makes the liquid among bubbles accumulate to lift the water level. Consequently, the detected local film thickness in the non-adiabatic experiment is almost the same or even thicker than that under adiabatic condition (region II in Fig. 8). When the film thickness decreases further, the generation of bubbles is restrained and finally ceases (region III in Fig. 8). Note that the liquid film gets ruptured with the thickness of a hundred micrometers. The effect of bubble generation on the critical film thickness can be ignored.

3. Results and discussions

3.1. Evolution of the liquid film

Fig. 10 shows the variation of the film thickness δ along the flow direction with different heat flux under the constant liquid and gas mass flow rates. Irrespective of adiabatic or non-adiabatic, the film thickness decreases along the flow direction due to the entrainment and evaporation (non-adiabatic). At a lower heat flux, the thinning process is mainly governed by the entrainment and the evaporation effect apparently becomes less pronounced. By increasing the heat flux, the effect of evaporation is observed to enhance gradually, leading to a rapid decrease in film thickness.

Fig. 11 shows the variation of the time-averaged film thickness under different gas and liquid mass flow rates till rupture occurs at the fixed measurement point 3. When liquid mass flow rate is low, the film thickness decreases almost linearly with the increasing gas velocity and the rupture occurs in a relative short time, indicating a nearly constant entrained rate. By increasing the liquid mass flow rate, the entrained rate seems decreases and the thinning process turns into a parabolic tendency. With the further increase in liquid mass flow rate, the film thickness firstly relative slowly decreases and then dramatically decreases with the increase of gas velocity (like cotangent image). In this case, the entrained rate firstly decreases and then increases with the increase in gas velocity. It is also worthwhile to mention that the averaged film thickness for an integrity film linearly increases with the increase in liquid mass flow rate.

3.2. Integrity of the liquid film

Fig. 12 shows the critical liquid film thickness for an integral film and its time-averaged value under various flow conditions. Without heating, the critical liquid film thickness remains almost the same for a specific surface, though the time-averaged film thickness grows with the increase in gas, and the liquid mass flow rates and the range of film thickness turn to be wider. i.e. the critical film thickness under adiabatic condition is ~111.51 μm (Fig. 12a). A similar conclusion is also drawn from non-adiabatic results (Fig. 12b). Thus, besides surface condition, the critical thickness for an integral liquid film is dominated by heat flux. Additionally, the critical film thickness and the time-averaged thickness

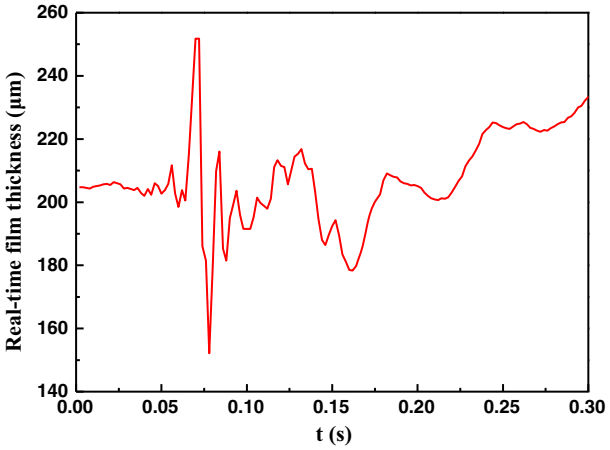

Fig. 9. Detected bubbles departure by optical sensor.

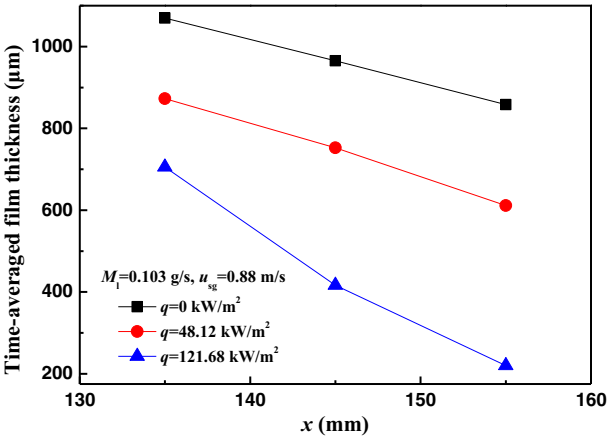

Fig. 10. Variations of the film thickness along flow direction.

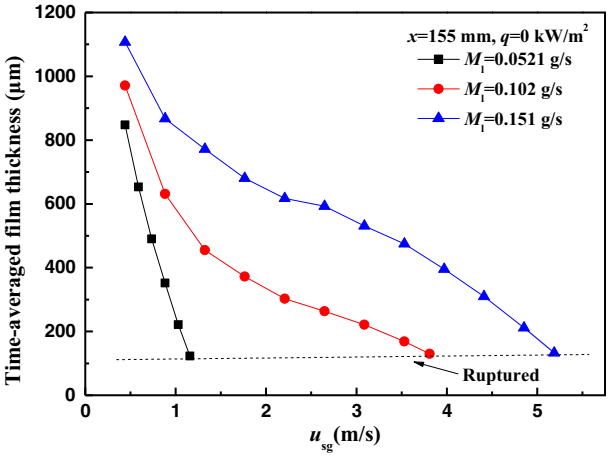

Fig. 11. Variations of the film thickness under different flow conditions.

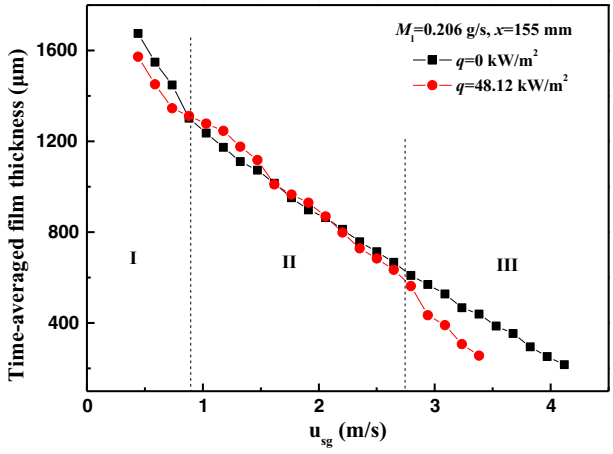

Fig. 8. Comparison of the film thickness between non-adiabatic and adiabatic conditions.

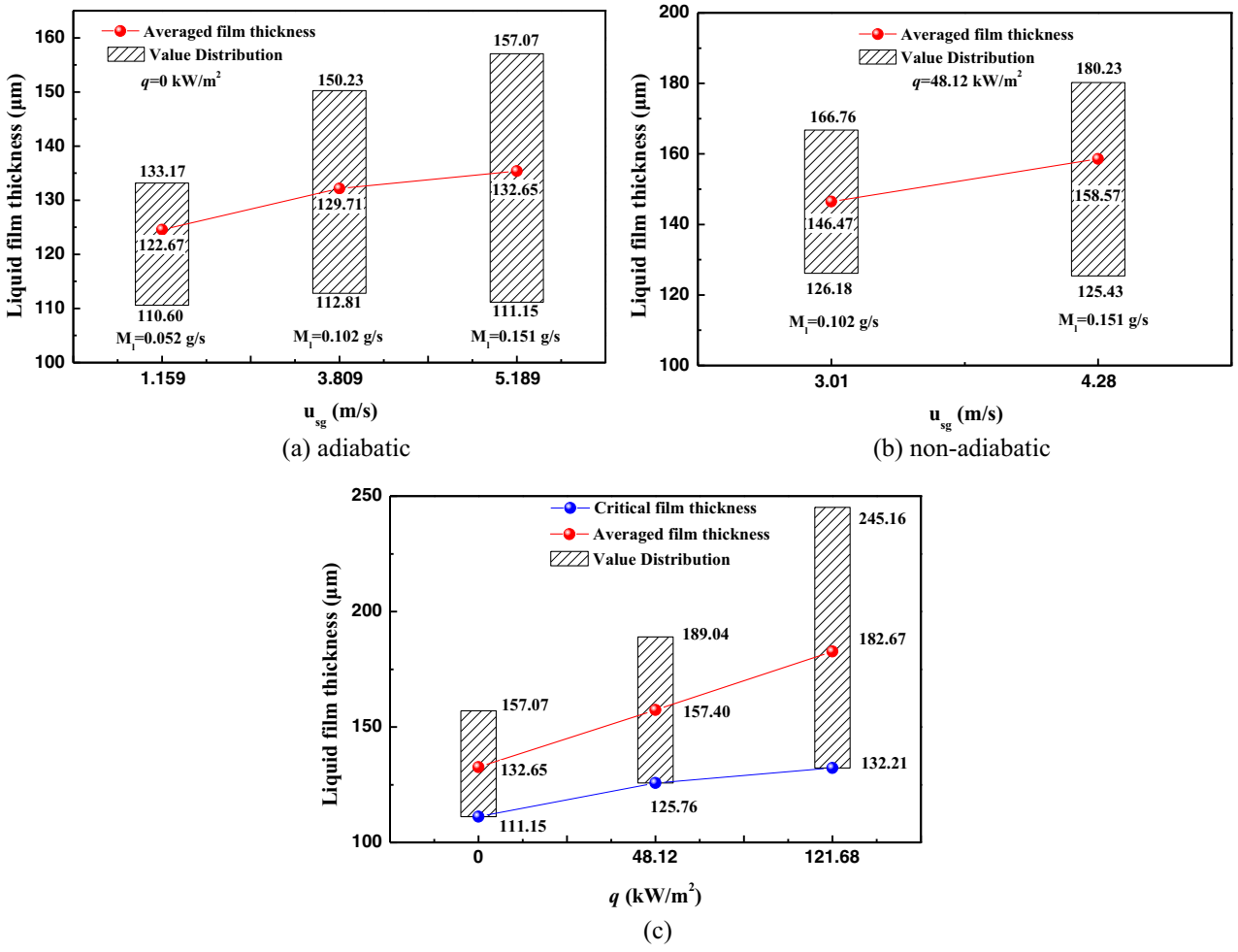

Fig. 12. Critical film thickness under different flow conditions.

increase with the increasing heat flux (Fig. 12c), indicating a more chaotic liquid film under high heat flux.

3.3. Film instability

The mechanism of the film rupture depends on the thickness of the liquid film present, since this determines if it is stable, metastable or unstable [29,30]. Generally, for a stratified flow, the gravity always acts as a stable factor, whereas the instabilities include film evaporation, shear driven interfacial instabilities such as Rayleigh-Taylor or Kelvin-Helmholtz waves, and interfacial deformation due to surface tension gradients arising from thermal or concentration gradients within the liquid film [31].

Fig. 13 shows the spectrum of the interfacial waves under different gas velocities and a constant liquid mass flow rate in adiabatic condition. A dominant wave frequency is observed to exist, indicating a period of fluctuation on the gas-liquid interface. Increasing the differential velocity between gas and liquid phases enhances the destabilizing Kelvin-Helmholtz instability which leads to a more "wavy" interface, i.e. the dominant wave frequency increases with the increase in gas velocity. It is also worthwhile to mention that the amplitude of the fluctuation decreases with the increase of gas velocity. Similarly, as seen in Fig. 14, increasing liquid mass flow rate increases the dominant wave frequency. The stabilizing effect of gravity increases with increasing film thickness, consequently resulting in a reduction in the amplitude of the fluctuation.

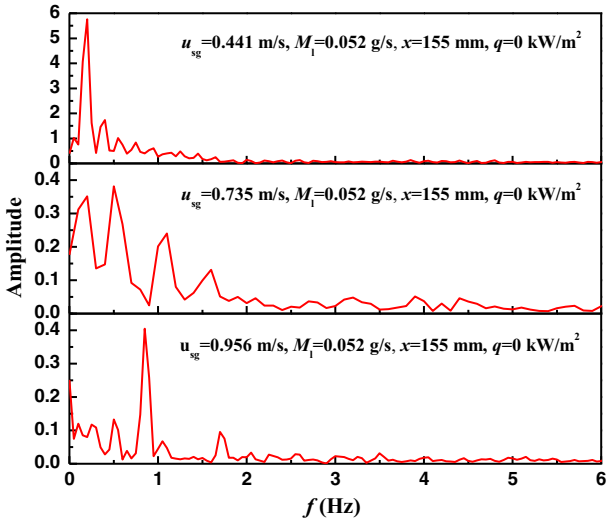

Fig. 13. Effect of the gas velocity on the film spectrum.

Fig. 15 shows the spectrum of the fluctuations when the film rupture is approaching. Here, the mixture velocity u_m ($u_m = u_g + u_l$) is employed. When the mixture velocity increases, the dominant wave frequency gradually disappears and the spectrum has multiple components and the relative strengths of each individual

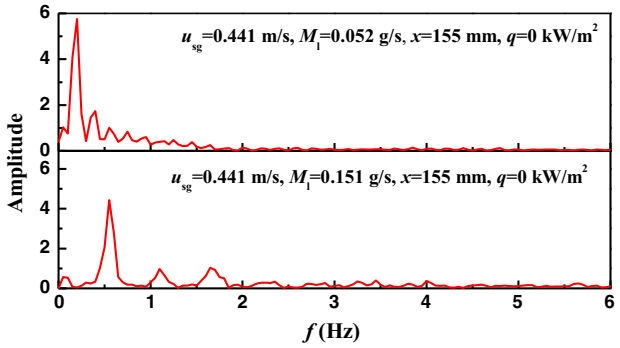

Fig. 14. Effect of the liquid mass flow rate on the film spectrum.

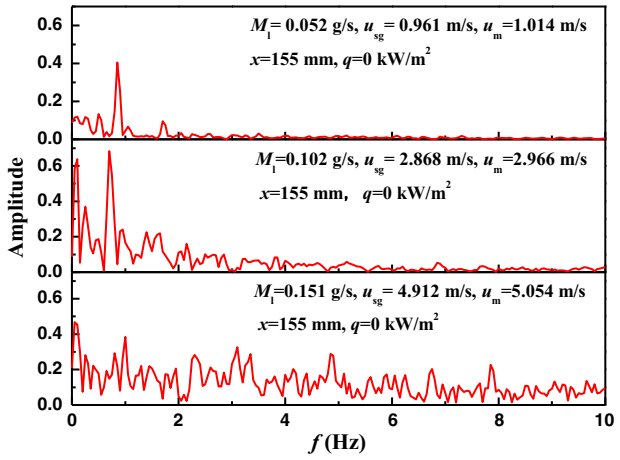

Fig. 15. Spectrum near rupture occurs.

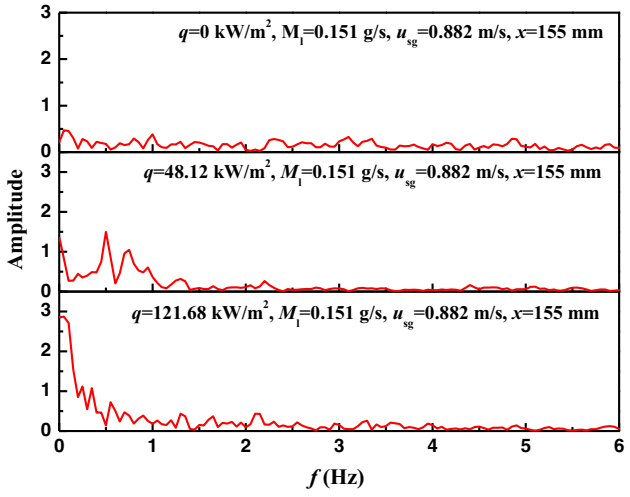

Fig. 16. Effect of heat flux on film spectrum.

frequency are similar, which indicates that the liquid film becomes more stable when the rupture occurs.

Fig. 16 shows the effect of heat flux on the film fluctuations under the constant liquid mass flow rate and gas velocity (e.g. M_l = 0.151 g/s, u_{sg} = 0.882 m/s). In adiabatic scenario, the liquid film relatively has multiple components and the frequencies have similar strength. Thus, the interface seems relative stable compared with the heating ones. Subsequently, parts of frequencies are restrained and gradually a dominant frequency appears and

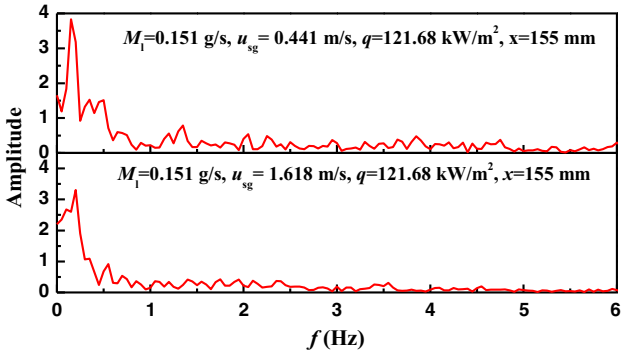

Fig. 17. Effect of gas velocity on film spectrum under higher heat flux.

enhanced when heat flux increases. When the heat flux increases to a higher level, the strong evaporation promotes an apparent periodical fluctuation with intensive amplitude. As discussed in Fig. 13, the dominant wave frequency increases with the increase in gas velocity. However, the effect of gas shearing will go away with an increase in the heat flux, as seen in Fig. 17. It can be anticipated that the effect of evaporation is more prominent for film instability when heat flux is high enough.

4. Conclusions

The present study investigates the hydrodynamics of a thin liquid film under the gas shearing and thermal influences. A new test rig is developed to investigate the dynamics of liquid film on the bottom of horizontal, rectangular channel, which is driven by the gas flow from above and heated from below. The detailed evolution of liquid film is discussed thoroughly. Due to the competitive relationship between the entrainment and evaporation, the film thickness varies linearly or nonlinearly under different flow conditions. Additionally, the occurrence of the liquid film rupture is random, and the critical thickness for an integral film is dominantly affected by the heat flux and increases with the increasing heat flux. We also employ the frequency spectrum analysis to the film instability to evaluate the factors and properties which govern film dynamics, stability and rupture. The results indicate that the effect of heat flux on film instability is more prominent when heat flux increases.

Acknowledgements

This study is supported by the NORTHNET program. The authors thank the staff at the Nuclear Power Safety Laboratory for their technical support in the experimental setup. This study was also supported by China National Funds for Distinguished Young Scientists under Grant No. 51425603 and the Science Foundation of China University of Petroleum, Beijing No. 2462016YJRC029.

References

[1] J.G. Collier, J.R. Thome, Convective Boiling and Condensation, Oxford University Press, 1994.
[2] S.G. Bankoff, Minimum thickness of a draining liquid film, Int. J. Heat Mass Transf. 14 (12) (1971) 2143–2146.
[3] J. Mikielewicz, J.R. Moszynski, Minimum thickness of a liquid film flowing vertically down a solid surface, Int. J. Heat Mass Transf. 19 (1976) 771–776.
[4] A.B. Ponter, K.M. Åswald, Minimum thickness of a liquid film flowing down a vertical surface-validity of Mikielewicz and Moszynskfs equation, Int. J. Heat Mass Transf. 20 (5) (1997) 575–576.
[5] A. Doniec, Flow of a laminar liquid film down a vertical surface, Chem. Eng. Sci. 43 (4) (1998) 847–854.
[6] D.T. Hughes, T.R. Bott, Minimum thickness of a liquid film flowing down a vertical tube, Int. J. Heat Mass Transf. 41 (2) (1988) 253–260.

[7] M.S. El-Genk, H.H. Saber, Minimum thickness of a flowing down liquid film on a vertical surface, Int. J. Heat Mass Transf. 44 (15) (2001) 2809–2825.
[8] A. Sharma, E. Ruckenstein, Dewetting of solids by the formation of holes in macroscopic liquid films, J. Colloid Interf. Sci. 133 (2) (1989) 358–368.
[9] A. Sharma, E. Ruckenstein, Energetic criteria for the breakup of liquid films on nonwetting solid surfaces, J. Colloid Interf. Sci. 137 (2) (1990) 433–445.
[10] A. Oron, S.H. Davis, S.G. Bankoff, Long-scale evolution of thin liquid films, Rev. Mod. Phys. 69 (3) (1997) 931–980.
[11] J.P. Burelbach, S.G. Bankoff, S.H. Davis, Nonlinear stability of evaporating/condensing liquid films, J. Fluid Mech. 195 (1988) 463–494.
[12] R.V. Craster, O.K. Matar, Dynamics and stability of thin liquid films, Rev. Mod. Phys. 81 (3) (2009) 1131–1198.
[13] A.K. Rajvanshi, J.S. Saini, R. Prakash, Investigation of macrolayer thickness in nucleate pool boiling, Int. J. Heat Mass Transf. 35 (1992) 343–350.
[14] T. Kumada, H. Sakashita, Pool boiling heat transfer-II. Thickness of liquid macrolayer formed beneath vapor masses, Int. J. Heat Mass Transf. 38 (1995) 979–987.
[15] Y.H. Zhao, T. Masuoka, T. Tsuruta, Unified theoretical prediction of fully developed nucleate boiling and critical heat flux based on a dynamic microlayer model, Int. J. Heat Mass Transf. 45 (15) (2002) 3189–3197.
[16] I.C. Bang, S.H. Chang, W.P. Baek, Visualization of a principle mechanism of critical heat flux in pool boiling, Int. J. Heat Mass Transf. 48 (2005) 5371–5385.
[17] A. Ono, H. Sakashita, Liquid-vapor structure near heating surface at high heat flux in subcooled pool boiling, Int. J. Heat Mass Transf. 50 (2007) 3481–3489.
[18] T.G. Theofanous, J.P. Tu, A.T. Dinh, T.N. Dinh, The boiling crisis phenomenon. Part I: nucleation and nucleate boiling heat transfer, Exp. Therm. Fluid Sci. 26 (2002) 775–792.
[19] T.G. Theofanous, J.P. Tu, A.T. Dinh, T.N. Dinh, The boiling crisis phenomenon. Part II: dryout dynamics and burnout, Exp. Therm. Fluid Sci. 26 (2002) 793–810.
[20] T.G. Theofanous, T.N. Dinh, High heat flux boiling and burnout as microphysical phenomena: mounting evidence and opportunities, Multip. Sci. Technol. 18 (3) (2006) 251–276.
[21] T.N. Dinh, J.P. Tu, The Micro-hydrodynamics that govern critical heat flux in pool boiling, in: International Conference on Multiphase Flow, ICMF 2007, Leipzig, Germany, July 9–13, 2007.
[22] S.J. Gong, W.M. Ma, T.N. Dinh, Diagnostic techniques for the dynamics of a thin liquid film under forced flow and evaporating conditions, Microfluid. Nanofluid. 9 (2010) 1077–1089.
[23] S.J. Gong, W.M. Ma, T.N. Dinh, An experimental study of rupture dynamics of evaporating liquid films on different heater surfaces, Int. J. Heat Mass Transf. 54 (2011) 1538–1547.
[24] S.J. Gong, W.M. Ma, L.X. Li, An experimental study on the effect of liquid film thickness on bubble dynamics, Appl. Therm. Eng. 51 (2013) 459–467.
[25] S.J. Gong, W.M. Ma, H.Y. Gu, An experimental investigation on bubble dynamics and boiling crisis in liquid films, Int. J. Heat Mass Transf. 79 (2014) 694–703.
[26] S.J. Gong, W.M. Ma, C. Wang, et al., An investigation on dynamic thickness of a boiling liquid film, Int. J. Heat Mass Transf. 90 (2015) 636–644.
[27] S.J. Gong, W.M. Ma, T.N. Dinh, Simulation and validation of the dynamics of liquid films evaporating on horizontal heater surfaces, Appl. Therm. Eng. 48 (2012) 486–494.
[28] R. Revellin, J.R. Thome, A theoretical model for the prediction of the critical heat flux in heated microchannels, Int. J. Heat Mass Transf. 51 (2008) 1216–1225.
[29] N. Borhani, B. Agostini, J.R. Thome, A novel time strip flow visualization technique for investigation of intermittent dewetting and dryout in elongated bubble flow in a microchannel evaporator, Int. J. Heat Mass Transf. 53 (2010) 4809–4818.
[30] N. Borhani, J.R. Thome, Intermittent dewetting and dryout of annular flows, Int. J. Multiph. Flow 67 (2014) 144–152.
[31] H.S. Kheshgi, L.E. Scriven, Dewetting: nucleation and growth of dry regions, Chem. Eng. Sci. 46 (1991) 519–526.